v. 14, n. 3, p. 7-15, 2025 ISSN 2237-9223



DOI: http://dx.doi.org/10.15260/rbc.v14i3.946

Use of 3D printed platform for GSR quantification using digital image analysis and smartphone.

A.S. Figueira ^{a,*}, F.F.C. Marques ^b, W.F. Pacheco ^c

- ^a Instituto de Criminalística Carlos Éboli (ICCE), Superintendência-Geral de Polícia Técnico-Científica (SGPTC), Secretaria de Estado de Polícia Civil do Rio de Janeiro (SEPOL), Rio de Janeiro (RJ), Brasil
- b Laboratório de Química Analítica Fundamental e Aplicada (LaQAFA), Instituto de Química, Universidade Federal Fluminense, Niterói (RJ), Brasil

*Endereço de e-mail para correspondência: <u>alessandro.figueira@pcivil.rj.gov.br</u>. Tel.: +55-22-981653044.

Recebido em 29/01/2025; Revisado em 30/07/2025; Aceito em 23/08/2025

Resumo

Para a determinação de resíduo de tiro (GSR) esparadrapo é comumente utilizado como base para aplicação do teste colorimétrico com rodizonato de sódio pela polícia. Neste contexto, este trabalho tem como objetivo quantificar o GSR depositado na mão de um atirador por meio de uma plataforma de impressão 3D utilizando análise de imagem digital e um smartphone. A metodologia baseiase no teste colorimétrico pela formação do complexo colorido de rodizonato de chumbo, tamponado com solução de tartarato em pH 2,40 e a quantificação se dá pela análise de sua imagem digital no software ImageJ, que gera histogramas contendo dados relativos à intensidade da cor de cada amostra. Curvas analíticas foram construídas correlacionando o sinal analítico com o GSR em termos de massa de Pb. O método foi aplicado em testes de tiro e mostrou-se eficaz após sucessivas adições cumulativas de Pb na mão do atirador, o que corresponde a 7 tiros consecutivos de pistola. Amostras de GSR geradas a partir de tiros de pistola calibre .380 mostraram massas de Pb de 2,42 μg, enquanto as amostras geradas após tiros de canhão antiaéreo mostraram massas de Pb de 1,38 μg a 1,49 μg. Espera-se que a utilização da metodologia possa auxiliar na elucidação de fatos criminosos através de um método rápido e de baixo custo.

Palavras-Chave: impressão 3D; resíduo de tiro; GSR; arma de fogo; imagem digital.

Abstract

For the determination of gunshot residue (GSR) adhesive plaster is commonly used as base to apply the sodium rhodizonate colorimetric test by the police. In this context, this work aims to quantify the GSR deposited on shooter's hand through a 3D printed platform using digital image analysis and smartphone. The methodology is based on the colorimetric test by the formation of the colored Pb–rhodizonate complex, buffered with tartrate solution at pH 2.40 and the quantification is given by the analysis of its digital image in the ImageJ software, which generates histograms containing data relating to the color intensity of each sample. Analytical curves were constructed correlating the analytical signal with GSR in terms of Pb mass. The method was applied in shot tests and proved to be effective after successive cumulative additions of Pb on shooter's hand, which corresponds to 7 consecutive shots of pistol. GSR samples generated from .380 caliber pistol shots showed Pb masses of 2.42 µg, while samples generated after anti-aircraft shots showed Pb masses of 1.38 µg to 1.49 µg. It is expected that the use of the methodology can help in the elucidation of criminal events through a quick and low-cost method.

Keywords: 3D printing; gunshot residue; GSR; firearm; digital imaging.

1. INTRODUCTION

In the global ranking of homicides, Brazil stands out as the country with the highest absolute number of homicides, highlighting a scenario of pervasive violence and revealing the fragility of public security systems [1]. Firearm-related crimes are particularly alarming, as

firearms are among the primary instruments used in violent acts. This underscores the urgent need for effective forensic tools to address the challenges posed by gun-related violence. In this context, ballistic studies play a pivotal role in forensic science, particularly through the examination of gunshot residue (GSR), which aids in identifying the shooter [2].

^c Laboratório Peter Sørensen de Química Analítica, Instituto de Química, Universidade Federal Fluminense, Niterói (RJ), Brasil

When traditional ammunition is used, the detonation process generates solid, spherical microparticles containing lead (Pb), barium (Ba), and antimony (Sb), which are considered the primary markers of GSR. These particles, resulting from the primer's combustion, are typically deposited on the hands, clothing, or nearby surfaces of the shooter [2]. Current methods for detecting Pb in GSR frequently employ Scanning Electron Microscopy (SEM), a highly sensitive technique that allows the identification and morphological characterization of particles. However, the high cost and technical demands of SEM limit its widespread use in forensic laboratories, particularly in regions with constrained resources [3,4].

To address these limitations, alternative methods have been developed, focusing on chemical techniques that offer rapid, low-cost, and easy-to-apply solutions [5–9]. Among these, colorimetric analysis has gained attention due to its simplicity and effectiveness. The formation of the Pb-rhodizonate complex, a red-colored compound, serves as a basis for such analyses, as shown in Fig. 1. [10–12].

Figure 1. Reaction of Pb-rhodizonate complex formation.

Digital image analysis (DIA) [13] represents a avenue for advancing GSR detection methodologies. First introduced in 1964 for converting medical images into digital data, this technique has evolved into a versatile and cost-effective tool for analytical chemistry. By capturing and analyzing images with devices such as smartphones, digital cameras, and scanners, DIA enables the quantification of color changes associated with chemical reactions [13,14]. Various software tools, including the freely available ImageJ [15,16], facilitate this process by converting color information into numerical data, which can then be analyzed quantitatively. This approach mirrors the principles of molecular absorption spectrophotometry, providing a robust framework for colorimetric analysis [17].

Although the sodium rhodizonate colorimetric technique has been formally discontinued as a recommended standalone method for GSR analysis by official technical recommendation issued on April 26, 2021, its application can still provide useful results when integrated with advanced analytical approaches. In this work, the traditional test is significantly improved through the application of systematic digital image analysis using the ImageJ software and smartphone-based image capture. This integration aims to overcome the limitations

of the standalone colorimetric method, enhancing reproducibility, sensitivity, and accessibility for forensic applications.

The aim of this study is to develop a novel method for quantifying GSR in terms of Pb mass using digital image analysis and a smartphone. To achieve this, a 3D-printed platform was designed to facilitate consistent image capture. Additionally, an optical box was constructed to standardize lighting conditions and minimize external variability. Key parameters affecting the formation of the Pb-rhodizonate complex were also optimized to enhance the reliability and reproducibility of the method. This innovative approach seeks to provide a cost-effective and accessible alternative for GSR analysis, with potential applications in forensic laboratories worldwide.

2. EXPERIMENTAL

2.1. Reagents and material

The reagents used included lead nitrate (purity \geq 99.99 %) and sodium tartrate (purity \geq 99.99 %), both obtained from Vetec (Brazil), nitric acid from Hexis (Brazil), and sodium rhodizonate (purity \geq 97 %) from Sigma-Aldrich (Brazil).

All solutions were prepared using ultrapure water (resistivity of 18 M Ω /mm) obtained through an Arium Comfort II System (Sartorius - Goettingen, Germany). pH measurements were performed using a DM-22 pH meter (Digimed, Brazil).

For the collection and complex formation of gunshot residue (GSR), 3D-printed platforms made of ABS, without additives used. The platform was built in the dimensions 2 cm x 2cm, with a width of 0,5 cm, and a pin of 3 cm to facilitate the handling and allowing the piece to fit into an appropriate support, as shown in Fig. 2.



Figure 2. 3D printed platform

The CAD file (in STL format) of the 3D-printed platform is available as supplementary material to this article, enabling full reproducibility of the experimental setup, using a GTMax3D Core A1 Dual printer (Brazil) equipped with two extruders and connected to the Simplify3D program to be tested as new substrates for GSR collection. Digital images were captured using an

iPhone-12 smartphone (Apple, USA).

For the tests, a Taurus PT 59S pistol, caliber .380 with a 19-round capacity, manufactured by Taurus (Brazil), and .380 ACP ammunition from CBC (Brazil) were used.

Additionally, a mobile anti-aircraft howitzer, M1 105 mm, manufactured by Springfield Armory (USA), was employed with AE M1 ammunition, caliber 105 mm, supplied by IMBEL (Brazil). Its specification is 18.5 kg in weight, 788 mm in length and 2.10 kg of TNT load weight.

Sample collection stages were carried out in two different installations: at Miracema Shooting Club and at the Brazilian Army Assessment Center (CAEx). The first is a shooting club, and the second is a Brazilian Navy base located on the edge of Guanabara Bay, both locations are in the state of Rio de Janeiro.

2.2. Instrumentation

Data acquisition during the preliminary studies in aqueous solutions was carried out using an Agilent Cary 60 UV-Vis spectrophotometer (Germany), equipped with a xenon light source and operating in reflection measurement mode. Measurements were performed using a quartz cuvette with a 1 cm optical path length, over a wavelength range of 190 to 1100 nm.

The optical box was constructed with a shoe box measuring 29.3 cm x 18.3 cm x 10.0 cm. Its interior was painted white to make it brighter and to reflect light efficiently. A tape of white LED (Light-Emitting Diode) was attached using hot glue to the inside of the box lid to maintain its standardized lighting. It was also necessary to adjust some parameters, such as the focal length and lighting and a hole was opened in the center of the upper external part of the box lid, so that a smartphone could be placed and photographs taken [18].

Figure 3 shows the optical box and Fig. 4 shows a schematic drawing of the phone on the box.



Figure 3. Optical box with its lid opened and LED lights on.

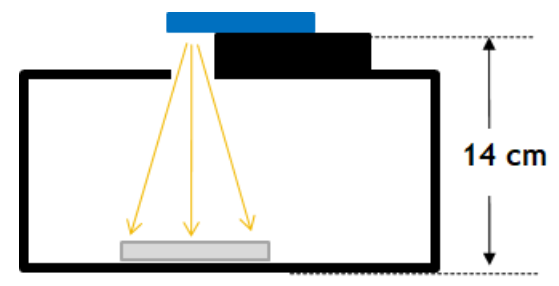


Figure 4. Schematic drawing of the phone on the optical box.

In this work, the ImageJ software based on the Java language was used. It is a program that can edit and handle images in a variety of formats. The software handles digital images, separating them into three color channels, corresponding to the colors of the RGB system (red, green and blue), generating histograms and statistical parameters for each channel [15,16].

The reference color channel used in this study is Green because that color is the complementary one to the red color of the Pb-rhodizonate complex. Moreover, the arithmetic mean of the green color histogram was used to calculate the analytical signal (Abs), according to Eq. 1.

$$abs = -\log \frac{P}{Po} \tag{1}$$

abs = absorbance

P = arithmetic mean of the histogram of each sample $P_o =$ arithmetic mean of the histogram of the blank

2.3. Statistical Analysis

Statistical analyses including the Fisher-Snedecor (F-test), Grubbs test, and ANOVA were performed using Python. These tests were used to verify the normality of calibration data, identify outliers, and assess the significance and fit of the analytical model. Confidence level was set at 95 %.

3. RESULTS AND DISCUSSION

3.1. Study of the 3D printed platform

A new alternative base to collect GSR was studied in this work. Platforms were printed with ABS, on GTMax3D Core A1 Dual printer, without additives, making light-colored resistant pieces, so as not to influence the colorimetric analysis. The reason for choosing ABS was to explore its viability sorving the metallic GSR particles trough coextraction with organic GSR, since particles as nitrocellulose, dinitrotoluene and nitroglycerin has interaction with the Styrene group of ABS. Beside this, the physical adherence of inorganic GSR particles may also be facilitated by surface roughness and electrostatic interaction.

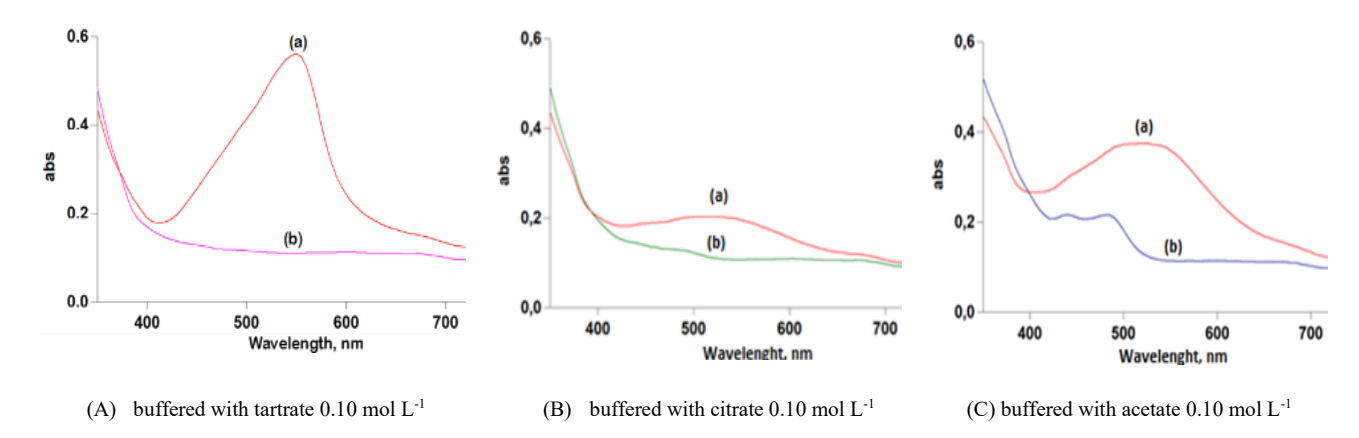


Figure 5. Molecular absorption spectrum in the UV-Vis region of rhodizonate solution 4.83 mmol L^{-1} buffered with: (A) tartrate 0.10 mol L^{-1} at pH 2.40; (B) citrate 0.10 mol L^{-1} at pH 2.40; and (C) acetate 0.10 mol L^{-1} at pH 2.40. All of them in the presence of 4.83 mmol L^{-1} of Pb²⁺.

3.2. Pb-Rhodizonate complex formation

The stability of the aqueous solution of Pb-rhodizonate complex has been studied with different buffers, such as tartrate, citrate and acetate [14].

In this work, a preliminary study was done to evaluate the intensity of the analytical signal and the stability of these buffers. For this purpose, different buffers at 0.1 mol L⁻¹ and pH 2.40 were analyzed in the UV-Vis region with rhodizonate 4.83 mmol L⁻¹ and 4.83 mmol L⁻¹ of Pb²⁺. The molecular absorption spectra of these complexes are shown in Fig. 5.

Among the three evaluated buffer systems – sodium acetate, sodium citrate, and sodium tartrate – the tartrate buffer produced the most intense molecular absorption spectrum for the Pb–rodizonate complex. This superior performance may be attributed to several factors.

Firstly, tartrate buffers typically operate within a slightly more alkaline pH range (around pH 5.0–6.5), which can enhance the stability of the rodizonate dianion,

promoting its availability for complexation. Secondly, tartrate ions possess multiple hydroxyl and carboxylate groups, allowing for moderate chelation of Pb2+ ions. Unlike citrate, which forms highly stable and multidentate complexes with Pb2+ – potentially sequestering the metal and preventing its interaction with rodizonate - tartrate appears to facilitate complexation without fully masking the metal ion. This intermediate complexation strength may favor the formation of the Pb-rodizonate complex in solution, leading to stronger absorbance signals. Additionally, tartrate may influence the local microenvironment in a way that enhances chromophore stabilization or reduces competing side reactions.

Once tartrate was defined as buffer to be used, its concentration was optimized in the range between 0.05, 0.10, 0.25, 0.50, 0.75, 1.00 and 1.25 mmol L⁻¹, keeping the concentration of Pb²⁺ and the concentration of rhodizonate at 4.83 mmol L⁻¹. The best result was obtained at 0.50 mmol L⁻¹, as shown in Fig. 6.

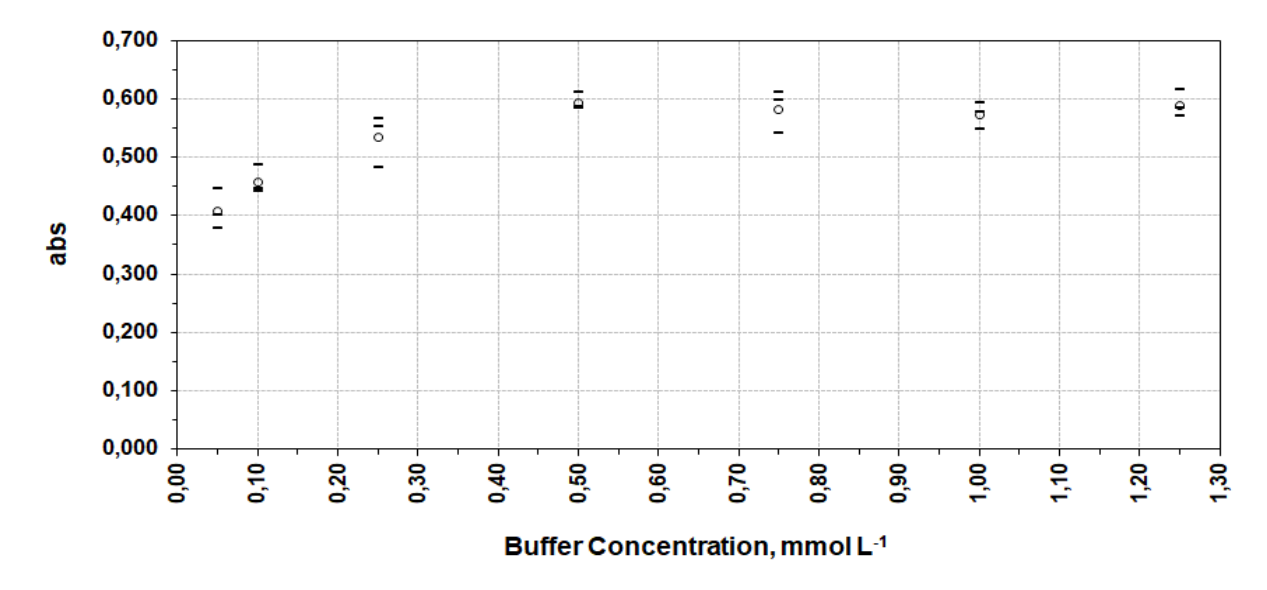


Figure 6. Molecular absorption results in the UV-Vis region for rhodizonate solution 4.83 mmol L⁻¹ buffered with different tartrate buffer concentrations at pH 2.40 in the presence of 4.83 mmol L⁻¹ of Pb²⁺.

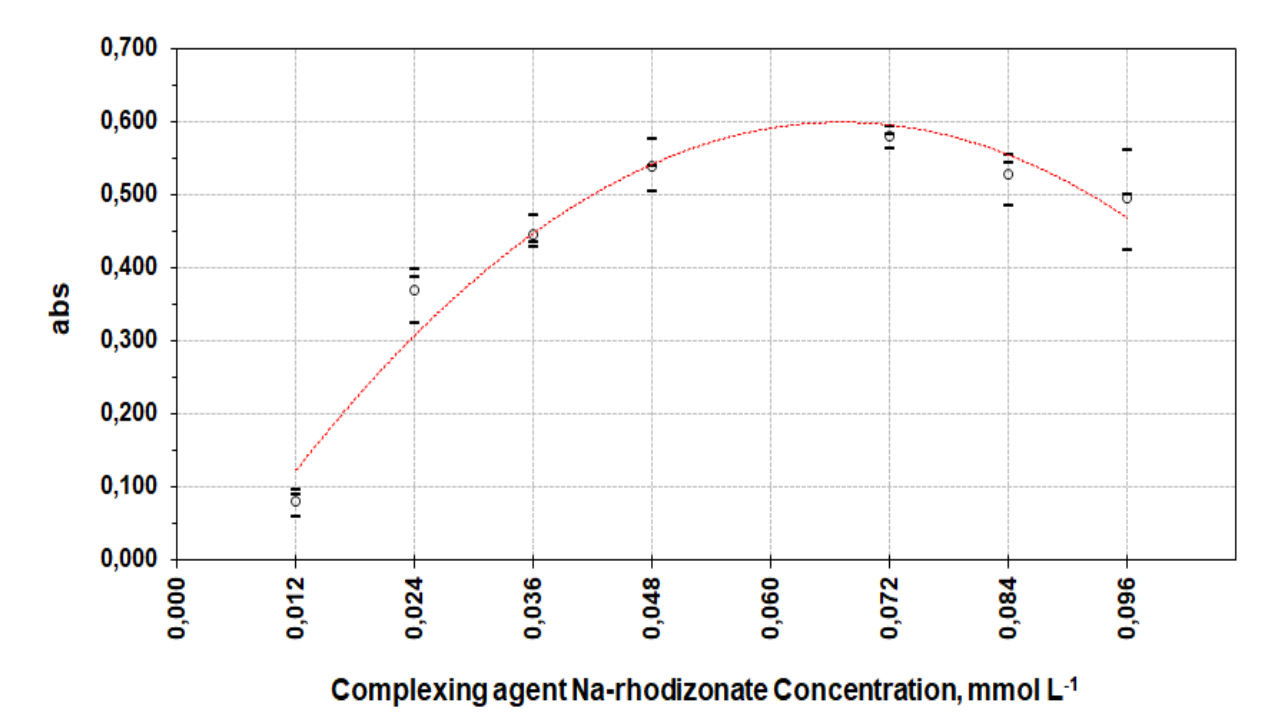


Figure 7. Molecular absorption results in the UV-Vis region for different concentrations of the complexing agent Na-rhodizonate buffered with tartrate buffer $0.50 \text{ mol } L^{-1}$ at pH $2.40 \text{ in the presence of } 4.83 \text{ mmol } L^{-1} \text{ of Pb}^{2+}$.

After the concentration of tartrate buffer is defined, the concentration of the complexing agent Na-rhodizonate was optimized by keeping the concentration of Pb²⁺ fixed at 4.83 mmol L⁻¹ and concentration of tartrate buffer fixed at 0.50mmol L⁻¹; varying the concentration of the complexing agent, in authentic triplicates each, at: 0.012, 0.024, 0.036, 0.048, 0.072, 0.084 and 0.096 mmol L⁻¹. The highest signal for absorbance at 550 nm was at 0.072 mmol L⁻¹, as shown in Fig. 7.

Beyond this concentration, a gradual decrease in absorbance was observed, suggesting a saturation point followed by a possible excess of ligand. This behavior may be attributed to two main factors: (i) the formation of secondary species (e.g., excess free rodizonate in solution absorbing at the same wavelength, contributing to background or spectral distortion), or (ii) a shift in complexation equilibrium due to ligand excess, potentially leading to less chromophoric species or weakly absorbing polynuclear complexes. Thus, 0.072 mmol L⁻¹ of Na-rodizonate was selected as the optimal concentration for subsequent analyses, providing the most intense and stable absorption signal for the Pb–rodizonate complex.

Although multivariate optimization techniques such as Response Surface Methodology (RSM) are widely employed in complex experimental systems, they were deemed unnecessary in this study. The parameters under investigation – buffer type and concentration, as well as complexing agent concentration – are chemically well-

defined and were individually optimized through a straightforward univariate approach. This strategy proved sufficient to achieve maximum analytical response and ensure method robustness, as demonstrated by the calibration curve and statistical validations

3.3. Construction of the analytical curve using the 3D platforms to collect standards samples

Aliquots of Pb^{2+} at 4.83 mmol L^{-1} solution, corresponding to masses from 1 to 7 μ g, were pipetted on laboratory watch glasses. After that, they were allowed to dry naturally, during 1 hour, at the temperature of 25°C, not exposed to the sun; and then, samples were collected using the 3D printed platforms, in authentic triplicates, as well as blank samples.

In each one, solutions under optimized conditions were added: tartrate buffer at 0.50 mmol $L^{\text{-1}}$ and complexing agent rhodizonate at 0.072 mmol $L^{\text{-1}}$.

After the Pb-rhodizonate complex formation, all platforms were immediately placed into the optical box and digital pictures were taken.

Figure 8 shows an example of digital images taken from Pb-rhodizonate complexes containing 4.0, 5.0, 6.0, 7.0 µg of Pb and the blank.

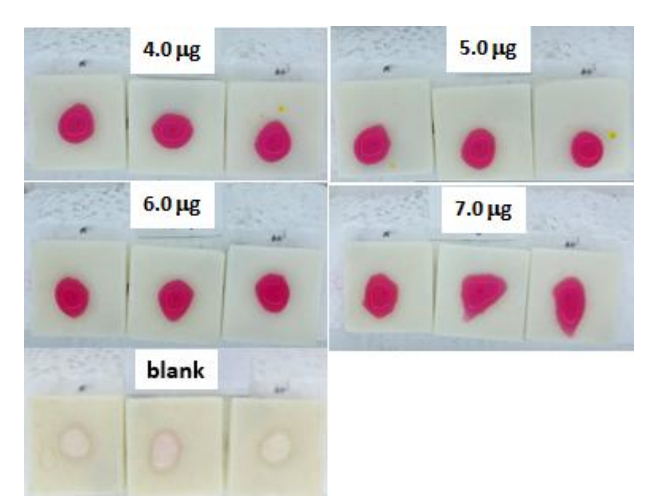


Figure 8. Pb-rhodizonate complexes formed on platforms containing 4.0, 5.0, 6.0, 7.0 μg of Pb and the blank.

Absorbance of the replicates was calculated, and their average was put on a chart, including the linear trend line, its equation and its determination coefficient (R^2) for the range of 1.0 to 7.0 µg of Pb (Fig. 9).

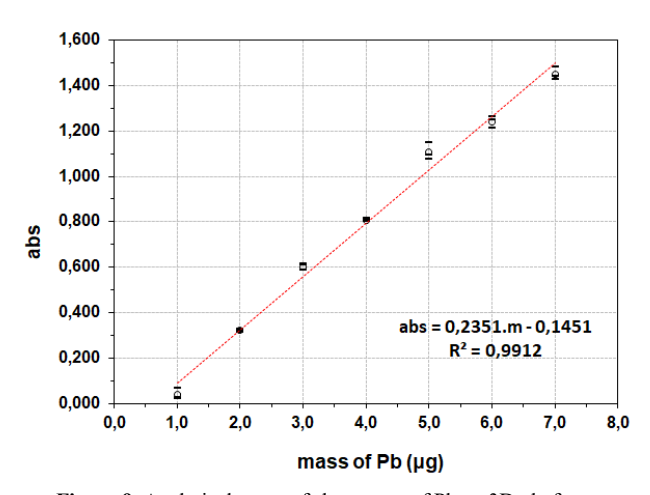


Figure 9. Analytical curve of abs x mass of Pb on 3D platforms

A normal distribution of the data obtained from a representative analytical curve (1.0–7.0 μg ; $R^2=0.9912$) was confirmed by the Fisher-Snedecor test (F-test) with a confidence level of 95 % and no outlier point was detected by the Grubbs test ($P \le 0.05$).

The statistical significance of the correlation between absorbance and mass of Pb was demonstrated by ANOVA (F = 563 > F tab = 10.01) and the lack of fit absence was also confirmed by ANOVA (F = 1.47 < F tab = 5.14), indicating a good suitability of the proposed mathematical model [19,20]. LOD was estimated by a S/N of 3:1, which corresponded to the lowest concentration of Pb that can be detected by the method and differentiated from the background noise of a blank matrix (free of analyte) [19,20].

In this study, LOD was calculated dividing the LOQ by the factor that relates these two limits, that is 3.33, and the results were 1.0 μ g and 0.30 μ g of Pb for LOQ and LOD, respectively.

3.4. Evaluation of Ba and Sb

It is known as "characteristic GSR" the one that contains solid particles of the metallic elements lead, barium and antimony simultaneously in their elemental forms [20]. For this reason, the evaluation of Ba and Sb as interfering agents and their impact on the formation of Pb-rhodizonate complex and on the application of the method were carried out.

According to the work of S.V.F. Castro and collaborators (2020) [21], in a GSR sampling after two gunshots, masses of Pb and Sb were analyzed and performed the determination through SWASV (Square Wave Anodic Stripping Voltammetry) by using Faraday's Law of Electrolysis. The metal masses were estimated at 1.7 ± 1.0 ng of Pb and 0.04 ± 0.02 ng of Sb.

In this study, known amounts of the target elements were deposited onto a touch plate to evaluate their influence on the Pb–rhodizonate complex formation. Specifically, 17.0 μg of Pb, 0.4 μg of Sb, and 0.4 μg of Ba were applied. Experiments were performed using: (i) Pb alone, (ii) Pb combined individually with either Sb or Ba, and (iii) Pb combined with both Sb and Ba. The amount of Pb was intentionally increased beyond the linear range (17.0 μg) to ensure the detection of potential interferences from Sb and Ba. Tartrate buffer and Narhodizonate solutions, previously optimized, were then added to promote the formation of the Pb–rhodizonate complex under controlled conditions.

Figure 10 shows the presence of red color, indicating that the formation of the complex occurs either when Pb is in the presence of the interfering agents Ba or Sb separately, and both interfering agents together, in proportional masses to those species found by S.V.F. Castro and collaborators (2020) [21].

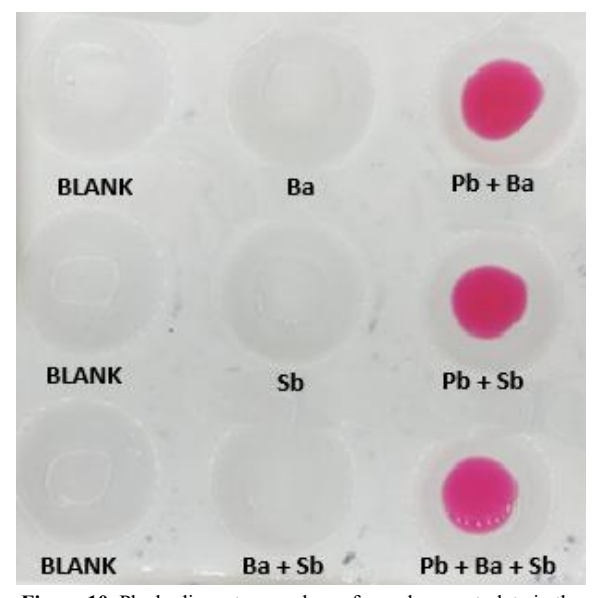


Figure 10. Pb-rhodizonate complexes formed on spot plate in the presence the interfering agents Ba and Sb separately and together.

3.5. Method application

The application of the method was carried out at the Miracema Shooting Club (CTM), located in the Northwest Fluminense region (Miracema-RJ, Brazil). The shooting range is an open space, at the time of the shooting it was a clear day, 25°C, without much wind.

The method was applied in a shot test, where GSR samples were collected from pistol after 1–7 shots, by successive applications of the platform on different regions of the shooter's right hand, such as palm, back, thumb and forefinger.

Figure 11 shows GSR sampling using the 3D platforms during a shot test.



Figure 11. GSR sampling using the 3D platforms.

A hand blank test was made before shots. The firearms were cleaned prior to each shot test to eliminate any possibility of contamination from previous discharges, and disposable gloves were worn at all times.

Initially, the shooter's hands were washed and dried with paper towel; then one shot was fired, and a sample was collected. After the first sample collection, the same washing procedure was performed. Similarly, the GSR samples were also collected after 2, 3, 4, and 7 shots.

All 3D printed platforms containing GSR samples were stored in plastic boxes with separate compartments to avoid contamination and loss of material.

The method was applied in a second shot test at the Brazilian Army Assessment Center (CAEx), where GSR samples were collected from shots of a mobile anti-aircraft howitzer 105 M1. The interest in applying the method in a large weapon was to compare the results with a pistol handgun. In this test, three different soldiers fired 10 consecutive shots each. At the end, a GSR sample was collected from the hand of each soldier.

Afterwards, all samples were taken to the laboratory to quantify GSR. The images of the Pb-rhodizonate complexes were analyzed in the ImageJ software, generating statistical data, and this data were used to calculate the amount of GSR in terms of Pb mass deposited in the shooter's hand, which was quantified, according to the analytical curve prepared for the shot test. All results of this study are shown in Table 1.

Table 1. Results for blanks and Pb-rhodizonate complexes from GSR samples of the pistol shots and anti-aircraft howitzer.

Shots	Type of gun	Calculated mass of Pb (µg)
1	pistol Caliber .380	< LOD
2	pistol Caliber .380	< LOD
3	pistol Caliber .380	< LOD
4	pistol Caliber .380	< LOD
7	pistol Caliber .380	2.42
10	anti-aircraft howitzer 105 M1	1.38
10	anti-aircraft howitzer 105 M1	1.39
10	anti-aircraft howitzer 105 M1	1.49

In the pistol study, identifiable lead signals were observed only after seven shots. Although the sensor proved viable, this result indicates that further studies are needed to increase the sorption capacity of the platform.

Although the anti-aircraft howitzer is a large-caliber weapon, the expected increase in Pb mass was not observed in the corresponding GSR samples. This result may be explained by multiple factors. First, the composition of military primers may differ significantly from those used in handgun ammunition, potentially generating lower amounts of lead-based residues. Second, the physical distance between the ignition point and the shooter's hand in heavy artillery operation may limit direct exposure to GSR. Finally, the use of protective gloves or equipment by military personnel could act as a barrier, reducing residue deposition on the skin. These combined factors may explain the unexpectedly lower Pb levels in the howitzer samples, independently of environmental variables.

Based on the results obtained, the method appears to perform more effectively for small-caliber semi-automatic firearms, such as the .380 pistol used in this study. The anti-aircraft howitzer, despite being a larger firearm, did not yield proportionally higher Pb residues. This suggests that the generation and deposition of GSR may vary significantly according to firearm design and ammunition characteristics. Therefore, the method shows higher applicability for personal firearms, where closer proximity between shooter and residue deposition surfaces favors detection.

4. CONCLUSIONS

This research found a new alternative base to collect and quantify GSR in terms of Pb mass, which is the 3D printed platform by using digital image analysis and smartphone. The study brought advances to the colorimetric test, maintaining its main characteristics such as easy applicability, quick response and low cost.

The method application in shot tests made it possible to conclude that the method is only effective after successive cumulative additions of Pb on shooter's hands, which corresponds to 7 consecutive shots of pistol Caliber .380. Although the method proved to be viable for determining lead residues, future studies will be carried out to modify the printed material with the aim of increasing its sorption capacity, and consequently, the sensitivity of the method.

The components used – optical box, smartphone, and open-source image analysis software – are compact and low-cost, enabling easy transportation and assembly in field conditions. While the current application was performed in a controlled laboratory environment, the system's portability makes it feasible for on-site forensic

analysis, providing faster results and minimizing the risk of contamination or evidence loss during transportation.

ACKNOWLEDGMENTS

The authors thank the Brazilian Army Assessment Center (CAEx) and the Miracema Shooting Club for the use of their installations.

The authors are grateful to FAPERJ (Fundação Carlos Chagas de Amparo à Pesquisa do Estado do Rio de Janeiro, Brazil), grants: E-26/211.186/2019, E-26/202.717/2019 and E-33/201.429/2022.

REFERENCES

- [1] Anuário de Segurança Pública de 2022, Fórum Brasileiro de Segurança Pública FBSP (2022).
- [2] Forensic Chemistry, By Suzanne Bell, 3rd Edition, CRC press (2022).
- [3] R.S. Nesbitt, e colaboradores, Detection of gunshot residue by use of the scanning electron microscope, Journal of Forensic Science: 595-610 (1976).
- [4] R.A. Costa, L.C. Motta, C.A. Destefani, R.R.T. Rodrigues, K.S. do Espírito Santo, G.M.F.V. Aquije, R. Boldrini, G.P.B Athayde, M.T.W.D. Carneiro, W. Romão, Gunshot residues (GSR) analysis of clean range ammunition using SEM/EDX, colorimetric teste and ICP-MS: A comparative approach between the analytical techniques, Microchemical Journal, 129: 339-347 (2016).
- [5] S. Rasheed, M. Ikram, D. Ahmad, M.N. Abbas, M. Shafique, Advancements in colorimetric and fluorescent-based sensing approaches for point-of-care testing in forensic sample analysis, Microchemical Journal, **206**: 111-438 (2024).
- [6] L.P. da Silva, L. Rodrigues e Brito, R.B. de Souza, C.F.P.M. Filho, V.B. dos Santos, L. Pinto, Screen-printed electrode modified with bismuth film and chemometric techniques for on-site detection and classification of gunshot residues, Forensic Chemistry, **38**: 100-563 (2024).
- [7] P. Shrivastava, S.K. Jain, N. Kumar, V.K. Jain, S. Nagpal, Handheld device for rapid detection of lead (Pb²⁺) in gunshot residue for forensic application, Microchemical Journal, **165**: 106-186 (2021).
- [8] G. Musile, Y. Agard, L. Wang, E.F. De Palo, B. McCord, F. Tagliaro, Paper-based microfluidic devices: On-site tools for crime scene investigation, Trends in Analytical Chemistry, **143**: 116-406 (2021).
- [9] A.T. Bruni, J.A. Velho, M.F de Oliveira, Fundamentos de Química Forense Uma análise prática da química que soluciona crimes, Ed. Millennium 228-243 (2012).
- [10] J.C.D. de Freitas, Identificação de assinaturas químicas em resíduos de disparos de arma de fogo em diferentes alvos, Instituto de Pesquisas Energéticas e

- Nucleares IPEN/SSP-SP, Dissertação de mestrado, (2010).
- [11] A. Duarte, Caracterização Elementar de Resíduos de Disparo de Armas de Fogo Gerados por Munição de Fabricação Brasileira, Universidade Federal do Rio Grande do Sul, Programa de Pós Graduação em Ciência dos Materiais, *Tese de Doutorado* 31-33 (2014).
- [12] R.S. Ledley, High-Speed Automatic Analysis of Biomedical Pictures, New Series, Vol. 146, **3641**: 216-223 (1964).
- [13] Y. Fan, J. Li, Y. Guo, L. Xie, G. Zhang, Digital image colorimetry on smartphone for chemical analysis: a review, Elsevier p. 4 (2021).
- [14] G.M. Fernandes, W.R. Silva, D.N. Barreto, R.S. Lamarca, P.C.F.L. Gomes, J.F. da S. Petruci, A.D. Batista, Novel approaches for colorimetric measurements in analytical chemistry: a review, Anal. Chim. Acta, p.187-203 (2020).
- [15] S.K. Kohl, J.D. Landmark, D.F. Stickle, Demonstration of Absorbance Using Digital Color Image Analysis and Colored Solutions, Journal of Chemical Education, Vol. 83, 4, p. 644 (2006).
- [16] Schneider, C. A., Rasband, W. S., & Eliceiri, K. W. NIH Image to ImageJ: 25 years of image analysis. *Nature Methods*, 9, 671-675 (2012).
- [17] W. da S. Lyra, V.B. dos Santos, A.G.G. Dionízio, V.L. Martins, L.F. Almeida, E. da N. Gaião, P.H.G.D. Diniz, E.C. da Silva, M.C.U. Araújo, Digital image-based flame emission spectrometry, Vol. 77, p. 1584-1589 (2019).
- [18] L.G.F Correia, N.F. Robaina, W.F. Pacheco, Desenvolvimento de metodologia analítica para detecção de resíduos de arma de fogo no corpo humano pela técnica de análise de imagem digital, Universidade Federal Fluminense, Graduação em Química Industrial, *Trabalho de Conclusão de Curso* (2019).
- [19] J.C. Miller, J.N. Miller, Statistics for Analytical Chemistry, 3° Ed. Ellis Horwoord (1993) p. 47-52.
- [20] INMETRO Documento DOQ-CGCRE-008 Orientação sobre Validação de Métodos Analíticos, Rev. 08 (2020).
- [21] S.V.F Castro, A.P. Lima, R.G. Rocha, R.M. Cardoso, R.H.O. Montes, M.H.P. Santana, E.M. Richter, R.A.A. Muñoz, Simultaneous determination of lead and antimony in gunshot residue using a 3D-printed platform working as sampler and sensor, Anal. Chim. Acta 1130 p. 126-136 (2020).